

Analysis of Glioblastoma Multiforme Tumor Metabolites Using Multivoxel Magnetic Resonance Spectroscopy

Meysam Siyah Mansoori^{1*}, Ayob Faramarzi¹, Karim Khoshgard^{2,3}, and Hadi Mozafari⁴

1. Department of Biomedical Engineering, Faculty of Medicine, Kermanshah University of Medical Sciences, Kermanshah, Iran

2. Pharmaceutical Sciences Research Center, Kermanshah University of Medical Sciences, Kermanshah, Iran

3. Department of Medical Physics, Faculty of Medicine, Kermanshah University of Medical Sciences, Kermanshah, Iran

4. Medical Biology Research Center, Kermanshah University of Medical Sciences, Kermanshah, Iran

Abstract

Background: Glioblastoma Multiforme (GBM) is the most common and deadly type of primary brain tumor in adults. Magnetic Resonance Spectroscopy (MRS) is a non-invasive imaging technique used to study metabolic changes in the brain tumors. Some metabolites such as Phosphocholine, Creatine, NAA/Cr, and Pcho/Cr have been proven to show a diagnostic role in GBM. The present study was conducted to analyze important metabolites using MRS multivoxel in GBM tumor.

Methods: In this study, information was collected from 8 individuals diagnosed with GBM using Siemens multivoxel MRS with a magnetic field strength of 3 T. Data were obtained by Point-Resolved Spectroscopy (PRESS) protocol with TE=135 ms and TR=1570 ms. NAA, Pcho, Cr, Ala, Gln, Gly, Glu, Lac, NAAG, and Tau metabolites were extracted and evaluated statistically.

Results: Given total number of normal voxels and total number of all voxels, levels of Cr, Glu, NAA, NAAG, and Gly/Tau ratio in healthy voxels were significantly higher than tumoral voxels ($p=0.005$, $p=0.03$, $p<0.001$, $p<0.001$ and $p=0.041$, respectively). In contrast, levels of Gly, Gln, Tau, Lac/Cr, Pcho/Cr, Pcho/NAA, Lac/NAA, and Gln/Glu ratios in tumoral voxels were significantly more than healthy voxels ($p=0.001$, $p=0.037$, $p<0.001$, $p=0.010$, $p<0.001$, $p<0.001$, and $p=0.024$, respectively). However, levels of Lac and Pcho had no significant difference in the two types of voxels.

Conclusion: In summary, compared to patients with glioblastoma with ¹H-MRS, the Pcho/Cr and Pcho/NAA ratios, and NAAG are the most important parameters to differentiate between tumoral and normal voxels.

Avicenna J Med Biotech 2020; 12(2): 107-115

Keywords: Glioblastoma multiform, Magnetic resonance spectroscopy, Neurochemical profiles, Voxel

Introduction

Glioblastoma Multiforme (GBM) is the most malignant and common tumor of central nervous system accounting for 40% of all types of brain tumors, among which 15 to 20% are of high grade^{1,2}. In 2017, more than half of 2607 patients with malignant brain tumor in the United States were diagnosed with GBM. Average survival time of patients with GBM under treatment and untreated patients is equal to 14.6 and 6.9 months, respectively, and the 5-year survival rate with treatment is reported as 9.8%³.

MRI as a non-invasive method is a suitable technique used to diagnosis of GBM tumor providing anatomical visualization of the brain tumor. In MRI images, GBM is seen as ring-enhancing lesions. However,

this pattern is not exclusive to GBM and is present in other diseases such as Tumefactive multiple sclerosis, abscess, and metastasis⁴. In spite of high contrast of soft tissue in MRI images for GBM tumor site, spatial spread of cerebral malignant cells is not detectable with MR modalities⁵. Distinction between healthy and tumoral areas is critical for treatment process including surgery, chemotherapy, or radiotherapy⁶.

Detailed information of brain tissue is needed to determine precise spatial location of the tumor. Neurological disorders alter concentration of metabolites such as Phosphocholine (Pcho), Creatine (Cr), and N-acetylaspartate (NAA) in brain tissue as well as concentration ratios of like NAA/Cr and Pcho/Cr. Biochemical pro-

* Corresponding author:
Meysam Siyah Mansoori, Ph.D.,
Department of Biomedical
Engineering, Faculty of Medicine,
Kermanshah University of
Medical Sciences, Kermanshah,
Iran
Tel: +98 83 34274618
Fax: +98 83 34276477
E-mail:
meysam.smansoori@kums.ac.ir
Received: 10 Apr 2019
Accepted: 6 Aug 2019

file of brain tissue including concentration and proportion of metabolites can be measured by non-invasive Proton magnetic resonance spectroscopy (1HMRS) ⁷.

Using a magnetic resonance imaging system and some hardware arrangements along with a software platform, Magnetic Resonance Spectroscopy (MRS) data can be obtained to calculate brain metabolites. MRS is applicable not only for hydrogen (¹H) but also on many other nuclei or isotopes like carbon (¹³C), nitrogen (¹⁵N]), fluorine (¹⁹F), sodium (²³Na), and phosphorus (³¹P). Abundant elements like hydrogen are used in brain imaging ⁸.

The first MRS report on the human brain dates back to 20 years ago ⁹. MRS has been applied to evaluate various types of brain tumors and has been proven as a part of clinical evaluation of the tumor ¹⁰. Einstein *et al* showed that patients with stereotactic radiosurgery have a longer survival for (Pcho/NAA) >2.1 than standard treatments ¹¹. Deviers *et al* found that concentration ratio of (Lac/NAA) >=0.4 in voxels prior to radiotherapy could be meaningfully used to predict recurrence of the tumor ¹².

Haaga *et al* introduced important brain metabolites such as NAA, Pcho, Lactate (Lac), Cr, Glutamic Acid (Glu), and Glutamine (Gln). Among them, the NAA metabolite has a vital importance in neurological diseases, especially brain tumors. They also reported that NAA/Cr and Pcho/Cr ratios in GBM tumor decreased and increased, compared to healthy tissue of the brain, respectively ⁹.

Parra *et al* found that distribution of metabolites such as NAA and Pcho in healthy and tumoral voxels showed a significant difference. On the other hand, concentration of NAA decreased and concentration of Pcho increased in tumoral voxels compared to healthy ones ⁵. Analyzing MRS data, Crain *et al* found that five ratios of Pcho/Cr, Cr/Pcho, Lac/Pcho, Lac/Lip and Lip/Lac are useful to differentiate between GBM healthy and tumoral voxels ⁷.

Various techniques have been implemented to quantify concentration of metabolites in MRS signals, but quantifications are still accompanied with high variations and big errors ¹³. Recent studies showed that, seemingly there are unknown metabolites or ratios, which need to be evaluated for GBM tumor using MRS multivoxel data. In this study, such ratios and metabolites were investigated.

Materials and Methods

General layout of this research is depicted in figure 1.

Data collection

Data related to 8 patients with GBM were obtained

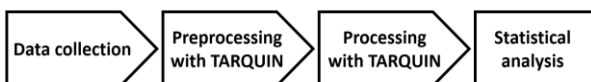


Figure 1. The study algorithm

at Imaging Center of Imam Khomeini Hospital in Tehran, Iran during March 2017 to March 2018. Before scanning, a complete explanation was given to all the subjects and ethical letters of consent were also signed. In addition, the data were obtained based on codes of the Medical Ethics Committee of Kermanshah University of Medical Sciences (Code of Ethics: IR.KUMS.REC.1397.142). Demographic information of studied patients is presented in table below.

In this study, imaging was performed through multivoxel Spectroscopy using a 3-Tesla MRI scanner made by Siemens Corporation. Multivoxel Spectroscopy was used to obtain a high-quality spectrum from a large area ¹⁴. The Point-Resolved Spectroscopy [PRESS] imaging protocol was used with following parameters: TE=135 ms, TR=1570 ms, and 1024 data points.

Magnetic field shimming was automatically performed before obtaining data. Long TE used for data collection in this study has several advantages over short TE: 1) in long TE, peak of lactate and alanine is better detectable than that of the fat compared to short TE and 2) NAA peak is distinguished from Glx (Glu or Gln) and the base line distortion reduces as well ¹⁵. Tagging and regionalization of tumoral and non-tumoral regions were performed using MRI data of the subjects by a radiologist at Imam Reza Hospital in Kermanshah, Iran.

Pre-processing

For pre-processing of the data, MRS range of imaging was determined using SIVIC; an open-source, standards-based software framework and application suite for processing and visualizing Digital Imaging and Communications in Medicine (DICOM), MR Spectroscopy data processing, and visualization. The MR image was subsequently overlaid on the MRS. Finally, the target region was determined (Figure 2).

The MRS signal obtained from device is a sinusoidal transient signal consisting of unwanted signals such as water signal, baseline signal, and residual signal (noise). The main signal received was defined as:

$$S [t]=Met[t]+w[t]+Res[t]$$

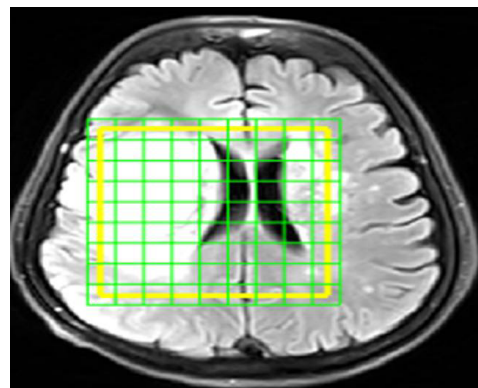


Figure 2. A sample of MRI image in SIVIC software in which the border of the tumor region at the time of imaging is determined as yellow box. Each green tagged square represents a voxel. The amount of each metabolite corresponding to each voxel is extracted in subsequent steps.

Where, S represents received signal, Met represents metabolites signal, w is water signal, and Res is residual signals including noise and other things.

The baseline signal originates from macromolecules, appearing at early stages in signal samples, and then rapidly disappears. The background signal is smooth. Like other MR imaging techniques, various artifacts such as Poor Shimming, Phasing Errors, and Chemical shift displacement influence Res signal quality^{16,17}. The main goal of pre-processing stage is finding signal of metabolites among the main signal and quantify metabolites with acceptable accuracy. For this reason, since levels of metabolites in brain tissue is much lower than water, water signal, which is 10,000 times larger than other metabolites¹⁸ must be suppressed. In the present study, water suppression was done with a frequency of 45 Hz. Figure 3A illustrates this step of pre-processing process.

Since the baseline signal has an undesirable effect on amount of other metabolites, to accurately calculate these values, the baseline signal should be reduced from the signal after water suppression (Figure 3B).

Processing

The Pcho, NAA, Cr, Lac, Gln, Glu, NAAG, Taurine (Tau), and Glycine (Gly) signals were selected as reference signals, since in TE=135 ms, the mentioned metabolites are measurable¹⁴. A sample of reference signals is displayed in figure 4A. Tarquin software fits (matches) the signal obtained from pre-processing stage with each reference signal individually¹⁹. By fitting the signals, the model's signal is obtained-the area below model curve for each metabolite is equal to its levels¹⁹. Fitting in Tarquin software was performed using LC model algorithm¹⁹. Figures 4B and 4C show software output after fitting. The area below the model diagram was calculated using Trapezoidal numerical integration method in Mathematics toolbox of MATLAB software.

Statistical analysis

Normal distribution of quantitative data was evaluated for two types of voxels by Kolmogorov-Smirnov test. Normal distribution of data was analyzed by Independent Samples T-test and non-normal distribution was assessed by Mann-Whitney U test. Pearson test was used to determine probable correlation of data in patients' voxels. Finally, sensitivity and specificity of

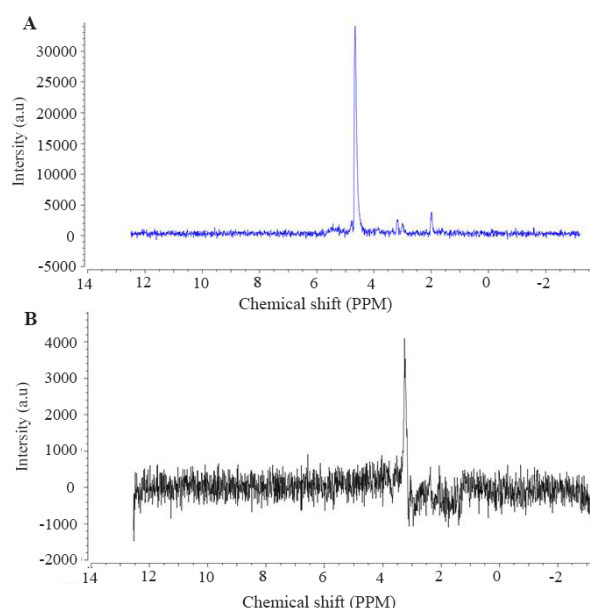


Figure 3. A) MRS signal information in a voxel before water suppression. As indicated, the high peak is related to water signal. The size of other metabolites is affected by the presence of water peak. The most important step in preprocessing phase is the removal of water signal. B) the signal obtained after the removal of the water peak. As each metabolite has a definite profile, the concentration of the metabolites is obtained from the peaks of this signal.

significant analytes were determined by drawing the ROC curve. In all calculations, level of significance was determined to be $p < 0.05$. To run statistical analysis for calculated levels from previous stage, SPSS software version 16 was used.

Results

In this study, 5 male and 3 female (Table 1) patients with GBM were studied by MRS test, and a number of 170 tumoral and 205 normal voxels were analyzed. Given total number of normal voxels and total number of all voxels, levels of Cr, Glu, NAA, NAAG, and Gly/Tau ratio in healthy voxels were significantly higher than tumoral voxels ($p=0.005$, $p=0.03$, $p<0.001$, $p<0.001$, and $p=0.041$, respectively; Table 2). In contrast, levels of Gly, Gln, Tau, Lac/Cr, Pcho/Cr, Pcho/NAA, Lac/NAA, and Gln/Glu ratios in tumoral voxels were significantly more than healthy voxels ($p=0.001$, $p=0.037$, $p<0.001$, $p=0.010$, $p<0.001$, $p<0.001$, and $p=$

Table 1. Information of the patients studied and the number of normal and tumoral voxels for each patient

Case number	Sex	Age	Number of scan	Normal voxel	Tumoral voxel
1	M	31	21	32	49
2	M	33	19	34	30
3	F	73	18	21	4
4	F	68	20	39	42
5	M	13	48	12	13
6	F	38	18	4	5
7	M	74	54	5	4
8	M	37	24	58	23

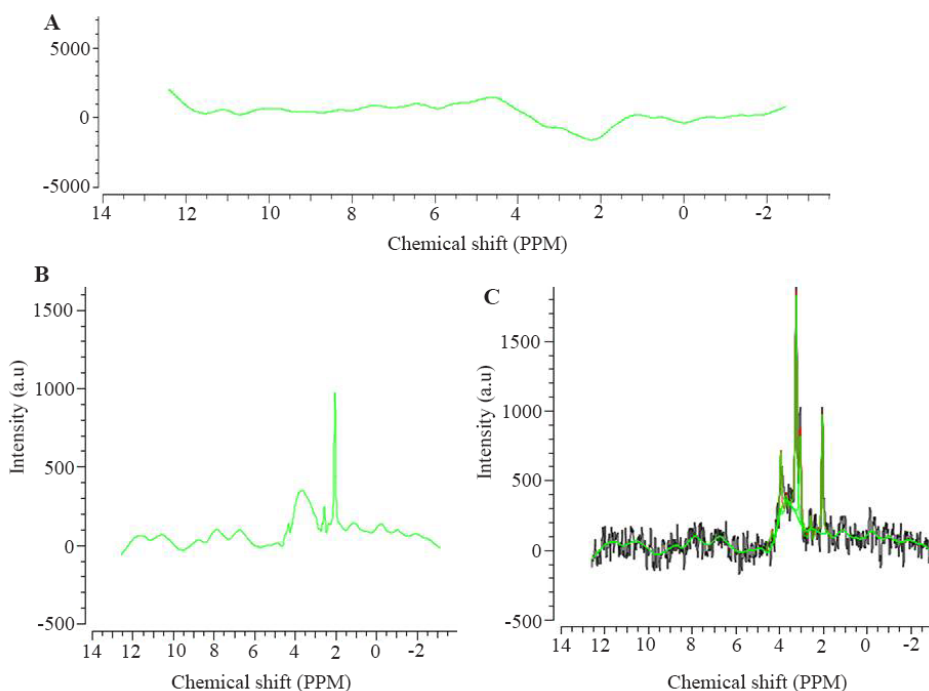


Figure 4. A) The baseline signal progonates from macromolecules. B) NAA signal selected as reference. C) Signal fitting is aimed at getting model signal from which concentration of metabolites can be calculated. The green curve shows the modeled signal.

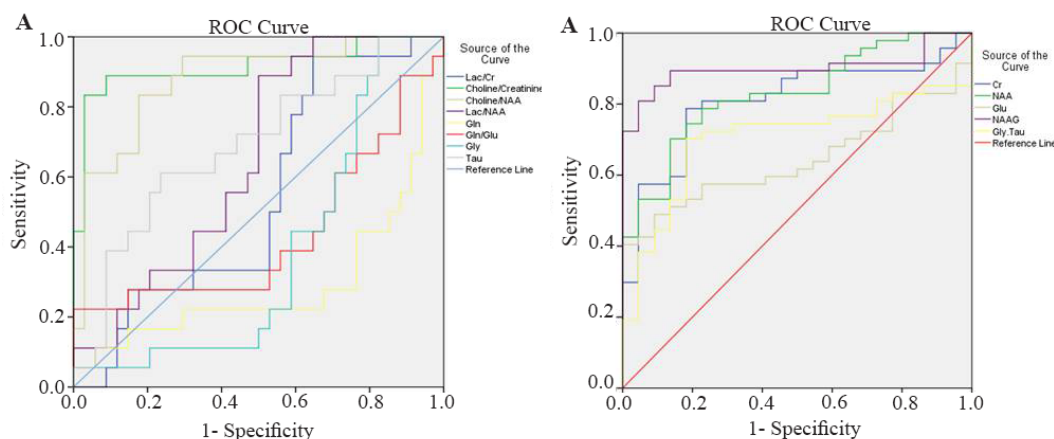


Figure 5. A) ROC curve for brain metabolites that were increased in tumor voxels. B) ROC curve for brain metabolites that were decreased in tumor voxels.

0.024, respectively; Table 2). However, levels of Lac and Pcho had no significant difference in the two types of voxels (Table 2). Results of correlation analysis between different biochemical parameters in tumoral voxels are shown in table 3. Finally, numerical values of sensitivity and specificity of different tests in detecting tumoral *vs.* normal voxels showed that Pcho/Cr had the highest diagnostic value with Area Under Curve (AUC) of 0.915 (sensitivity 83.3% and 97.1% specificity). The second suitable test was Pcho/NAA with AUC of to 0.879 (sensitivity 94.4% and 70.6% specificity). Third suitable test was NAAG with AUC of 0.845 (sensitivity 90.9% and 82.4% specificity) (Table 4, Figure 5).

Discussion

In this study, for the first time, diagnostic value of detectable metabolites in long TE was investigated by simultaneous analysis of several analytes in a combination of healthy and tumoral voxels. Our results showed that, levels of Cr, Glu, NAA, NAAG, and Gly/Tau ratio in healthy voxels were significantly higher than tumoral voxels. In contrast, levels of Gly, Gln, Taurine, Lac/Cr, Pcho/Cr, Pcho/NAA, Lac/NAA, and Gln/Glu ratios in tumoral voxels were significantly higher than healthy voxels.

Different biochemical analytes have a diagnostic application in various diseases. A biomarker is a biochemical molecule measured by definite protocol to

Table 2. The main MRS analysed parameters of tumor and normal voxels

Parameter	Statistical Information	Tumor Voxel (n = 170)	Normal Voxel (n = 205)	p-value
Creatine (Cr)	Mean±SD	45243.8±40989.9	56784.1±25570.4	0.005
	Median (IQR)	62577.9 (37197.7-78336.9)	52713(35942.1-70079.7)	NS
Phosphocholine (Pcho)	Range	383-382873	3145-188266	
	Median (IQR)	13597 (9052.4-24418.5)	18002.6 (9811.4-33567.7)	0.030
Glutamic Acid (Glu)	Range	1089-152550	2750-98338	
	Median (IQR)	10588.4 (3343.03-19059.5)	6886.6 (4034.05-12181.6)	0.037
Glutamine (Gln)	Range	2-142141	379-71261	
	Median (IQR)	11248 (5406.1-19704.3)	8065.3 (4565.7-12307.8)	0.001
Glycine (Gly)	Range	310-747186	272-78921	
	Median (IQR)	0.43 (0.24-1.21)	0.30 (0.17-0.79)	0.024
Gln/Glu Ratio	Range	0.00-8.85	0.00-6.33	
	Median (IQR)	8433.90 (4092.6-12953)	7113.60 (3294.8-15763)	NS
Lactate (Lac)	Range	270-85124	190-77207	
	Median (IQR)	0.15 (0.08-0.37)	0.12 (0.05-0.25)	0.01
Lac/Crea Ratio	Range	0.01-9.09	0.01-1.72	
	Median (IQR)	1.58 (1.18-2.39)	0.94 (0.74-1.17)	<0.001
Pcho/Crea Ratio	Range	0.04-7.34	0.31-2.82	
	Median (IQR)	28954 (12760-57837)	57739.8 (28379.4-77123)	<0.001
N-Acetylaspartate (NAA)	Range	2067-98759	2010-124864	
	Median (IQR)	1.95 (1.21-4.93)	0.93 (0.67-1.32)	<0.001
Pcho/NAA Ratio	Range	0.01-30.92	0.16-29.29	
	Median (IQR)	0.21 (0.11-0.52)	0.13 (0.05-0.25)	<0.001
Lac/NAA Ratio	Range	0.01-6.41	0.01-1.88	
	Median (IQR)	22160.7 (13330.5-44833)	50257.7 (28116-69125.1)	<0.001
N-Acetylaspartylglutamic acid (NAAG)	Range	1900-193971	865-130222	
	Median (IQR)	7144.4 (3408.4-12455.7)	4911.05 (2635.6-6744.3)	<0.001
Taurine (Tau)	Range	447-272522	51-32593	
	Median (IQR)	1.21 (0.81-2.18)	1.85 (1.16-3.85)	0.041
Gly/Tau Ratio	Range	0.31-102.66	0.08-70.86	

NS: Nonsignificant.

determine a pathologic process or responses to a therapeutic agent²⁰.

Kinoshita Y *et al*²¹ reported that, concentrations of choline-containing compounds, inositol, alanine, Gly, and phosphorylethanolamine increased in glioblastoma with respect to degree of malignancy. In particular, they detected a large amount of Tau in medulloblastoma. However, they found that total Cr concentrations decreased in nonneuroectodermal tumors. Similarly, we detected lower amounts of Cr and higher concentrations of Tau in tumor voxels rather than normal ones.

Consistent with our results, Righi *et al* showed higher levels of Gly in tumor biopsies than the controls. Additionally, Gly levels significantly increased in brain metastases and GBM biopsies²².

Different studies reported that higher activity of serine hydroxymethyltransferase or deficiency of hypoxanthine-guanine phosphoribosyltransferase in the gliomas tumor cells leads to high Gly levels. Even increased glycine peak is a differentiating agent for differentiation of glioblastoma from metastatic lesions¹⁵.

Moreover, increased Tau is seen in medulloblastoma, pituitary microadenoma and metastatic renal cell carcinoma. In the retinoblastomas, retina has the highest levels of Tau due to its high affinity transport system¹⁵. While, we found significant decreased ratio of Gly/Tau in tumor voxels rather than normal voxels. More studies are needed to determine role of both metabolites in glioblastoma.

However, Cr levels reduce about 15-40% in glial tumors or meningotheiomatous meningiomas. Also, in brain metastases, total Cr content is significantly lower compared to neuroectodermal tumors¹⁵. Cr is an important cellular energy metabolism metabolite. Despite of its stability in some pathological reactions influencing central nervous system, it typically decreases in glioblastoma and astrocytomas^{15,23}. Possibly, higher metabolism of tumor cells leads to a decrease in the Cr levels.

Preul *et al* showed that, signal intensities of lactate, NAA, Cr, and alanine can be applied in determining various grades of glioma²⁴. Our results showed that,

Table 3. Significant correlations between different parameters of Tumor voxels

Parameter	Statistic index	Pcho	Glu	Gln	Gly	Gln/Glu	Lac	Lac/Cr	Pcho/Crea	NAA	Pcho/NAA	Lac/NAA	NAAG	Tau
Cr	r ^a	0.755	0.732	0.589	0.729	NS	NS	NS	-0.451	0.714	-0.26	-0.368	0.563	0.261
	P ^b	<0.001	<0.001	<0.001	<0.001				<0.001	<0.001	0.019	0.001	<0.001	0.031
Pcho	r	1	-0.264	NS	0.799	0.384	-0.314	-0.444	NS	0.341	NS	-0.271	NS	NS
	P		0.031		<0.001	0.002	0.007	<0.001		0.002		0.030		
Glu	r	-	1	0.668	0.405	NS	0.403	0.402	-0.344	0.234	NS	NS	0.712	NS
	P			<0.001	<0.001		<0.001	0.001	0.006	0.045			<0.001	
Gln	r	-	-	1	0.393	0.337	0.628	0.294	NS	NS	NS	0.258	0.230	NS
	P				<0.001	<0.001	<0.001	0.008				0.025	0.015	
Gly	r	-	-	-	1	0.312	NS	NS	NS	0.440	NS	NS	0.222	0.728
	P					0.009				<0.001			0.036	<0.001
Gln/Glu	r	-	-	-	-	1	0.368	NS	NS	NS	NS	NS	NS	NS
	P						0.001							
Lac	r	-	-	-	-	-	1	0.702	NS	NS	NS	0.307	0.269	0.429
	P							<0.001				0.004	0.005	<0.001
Lac/Cr	r	-	-	-	-	-	-	1	NS	NS	NS	0.265	0.235	0.515
	P											0.025	0.034	<0.001
Pcho/Crea	r	-	-	-	-	-	-	-	1	-0.524	0.451	0.389	-0.309	NS
	P									<0.001	<0.001	0.002	0.005	
NAA	r	-	-	-	-	-	-	-	-	1	-0.539	-0.426	0.375	0.304
	P										<0.001	<0.001	<0.001	0.021
Pcho/NAA	r	-	-	-	-	-	-	-	-	-	1	0.607	NS	NS
	P											<0.001		
Lac/NAA	r	-	-	-	-	-	-	-	-	-	-	1	NS	NS
	P													
NAAG	r	-	-	-	-	-	-	-	-	-	-	-	1	0.303
	P													0.009

NS: Non significant; a) r coefficient; b) p-value.

Table 4. Diagnostic value analysis for significant different data between tumor and normal voxel

Parameter	AUC	Cut-off	Sensitivity (%)	Specificity (%)
Cr	0.727	50456	72.7	70.6
Glu	0.476	11975	54.5	47.1
Gln	0.291	4585	44.4	23.5
Gly	0.381	4540	83.3	23.5
Gln/Glu	0.435	0.279	66.7	23.5
Lac/Cr	0.544	0.083	66.7	44.1
Pcho/Cr	0.915	1.34	83.3	97.1
NAA	0.759	43397	72.7	76.5
Pcho/NAA	0.879	0.926	94.4	70.6
Lac/NAA	0.650	0.847	88.9	50
NAAG	0.845	32059	90.9	82.4
Tau	0.690	0.409	83.3	44.1
Gly/Tau	0.674	1.14	81.8	70.6

NAA levels decreased in tumoral voxels compared to normal ones. NAA as the second most abundant amino acid in the brain markedly decreases or is absent in malignant or benign tumors involving axonal loss. Apparently, absence of NAA biosynthetic enzyme (aspartate N acetyltransferase) in brain tumors is main cause of NAA signal loss¹⁵.

NAA is one of the most abundant amino acid derivatives in the brain and is considered as a source of metabolic acetate in brain cells. Levels of both NAA and NAAG decreased in glioma tumors. It is assumed that NAA hydrolysis provides high levels of acetate molecules used for lipogenesis in glioma tumor cells²⁵.

Lower levels of NAAG were found in tumoral voxels rather than normal voxels. This molecule is formed in neurons from NAA by adding glutamate residue and is degraded only in astrocytes. Both NAA and NAAG have important role in cell-specific glial signaling. They are important in function and development of brain, regulation of interactions of brain cells, maintenance of nervous system, and even as a neurotransmitter in CNS acting as a partial agonist of N-methyl-d-aspartate receptors. NAAG has an essential role in glial cell metabolism. In addition, NAAG aciduria has been detected in Canavan disease as neurodegenerative disease^{26,27}. Recently, a study suggested that astrocytes, oligodendrocyte progenitor cells, and neural stem cells could all serve as the cell of origin for glioblastoma occurrence²⁷. Probably, decreased level of NAAG has a causative metabolic and signaling effect on glioblastoma development.

Simultaneously, lower levels of glutamate and higher levels of glutamine were found in tumoral voxels compared to normal voxels. In this line, NAAG can also serve as a cellular storage for glutamic acid. On the other hand, Glu is converted into Gln returning to neurons by astrocytes²⁶. This reaction may lead to decreased Glu levels and increased Gln levels.

Furthermore, a part of Glu enters to Krebs cycle *via* converting to α -ketoglutarate for ATP production²⁸. Increased level of Gln in glioblastoma is possibly due to higher energy demand of tumor cell²⁹ and higher activity of glutamine synthase. Apparently, increased uptake of glutamine and its changing to glutamate is an important process in highly proliferated tumor cells³⁰.

Our results showed that Pcho level was the same between tumoral and normal voxels. Nevertheless, two different studies have reported that, Choline Kinase in several brain tumors is overexpressed and increased choline peak reflects increased cell membrane synthesis, turnover, and integrity¹⁵. Nelson *et al* indicated that an increase in the choline and a decrease in the NAA is so important to determine spatial extent of metabolic abnormality and consequent tumor activity³¹. Similarly, another study revealed a significant decrease in the NAA signal intensity in diaschitic cerebellar hemisphere and an insignificant decrease in the choline and Cr signal intensities.

Possibly, increased levels of choline are associated with cell proliferation, while NAA is a marker for density and viability of neurons³². More studies are required to clarify exact role of choline changes in tumor metabolism.

In our study, lactate levels of both tumoral and normal voxels were similar. However, increased rates of lactate production were reported. Also, lactate level was found to be associated with a range of tumors and tumor grade or tumor metabolic activity. In this line, lactate peak was found to be usually absent in low - grade brain tumors. It increases in high-grade primary brain tumor¹⁵. Likely, this difference may be due to differences in ethnicity or our small sample size.

Different reduced or increased ratios of glioblastoma biomarkers have pivotal role in diagnosis. In another study³³, in recurrent glioma tumor, Pcho/NAA and Pcho/Cr ratios were significantly higher than in radiation injury. However, NAA/Cr ratio was lower in recurrent glioma tumor than in radiation injury. Besides, in radiation injury, Pcho/Cr and Pcho/NAA ratios were significantly higher compared to normal-appearing white matter, and NAA/Cr ratio was lower in radiation injury than in normal-appearing white matter.

Tumoral voxels in our study were found to have higher NAA/Pcho compared to normal voxels, which is consistent with some studies^{23,32,34,35}. Pcho/NAA has been described as suitable biomarker of tumor prognosis and monitoring of treatment response. Similarly, Bulik *et al* illustrated that in recurrence glioblastoma at N-acetylaspartate ≤ 1.5 mM, Pchoe/N-acetylaspartate ≥ 1.4 , both sensitivity and specificity were equal to 100 and 91.7%, respectively³⁴.

Receiver operating characteristic analyses performed in the present study for assessment of NAA/Pcho ratio revealed that at 0.922 as cut-off, AUC was equal to 0.879 and sensitivity and specificity were equal to 94.4 and 70.6%, respectively. Ratai *et al* reported lower AUC in tumor (AUC=0.83) and higher AUC in peritumoral regions (AUC=0.95)²³. However, Tomas *et al*³² reported on Pcho/NAA ratio with highest significant sensitivity and specificity for glioblastoma recurrence (AUC=0.993; sensitivity of 100.0% and specificity of 94.7%). Furthermore, they reported on Pcho/Cr ratio with a weak sensitivity and specificity (74.6 and

63.2%, respectively; AUC=0.691)³². In contrast, our results demonstrated that, assessment of Pcho/Cr ratio was the best test for differentiation between normal and tumoral voxels. It had AUC equal to 0.915 at 1.34 as cut-off with 83.3 and 97.1% as sensitivity and specificity, respectively. Nevertheless, Ando *et al*³⁶ reported that, despite of significant higher ratio of Pcho/Cr in cases with residual/recurrent tumors than in non-neoplastic lesions; at point of 1.5 as cut-off, its sensitivity and specificity was equal to 64 and 83%, respectively. Presumably, this difference in sensitivity and specificity results of AUC is related to different technical details and differences in studied sample size.

Finally, in a systematic review, seven studies were reviewed including a total of 261 patients with high - grade glioma³⁷. Analysis showed that in peritumoral tissue pooled sensitivity/specificity of Pcho/NAA and Pcho/Cr ratio were equal to 0.85/0.93 and 0.86/0.86, respectively. Likewise, Pcho/NAA ratio had higher value of AUC and higher specificity rather than Pcho/Cr ratio in peritumoral region. They suggested that Pcho/NAA ratio of peritumoral region should be applied to increase accuracy of MRS to differentiate high-grade gliomas from metastases.

Ratai *et al*²³ reported that, Lac/Cr ratio in tumor was an important negative predictor of 6-month progression free survival. They also demonstrated that poorer outcome was associated with higher Lac/Cr. (AUC=0.79)²³. Our results indicated that, Lac/Cr ratio AUC was equal to 0.544, showing this index is weaker biomarker for glioblastoma rather than Pcho/NAA.

There were some limitations in our study. Following up the patients was not possible because, they often did not refer again to the center. In addition, sample size of the study was small. However, the subjects were selected during 18 months. Certainly, similar studies in larger scale and with larger sample size could be useful for better determination of ¹H-MRS power to detect GBM.

Conclusion

In summary, results of the current study showed that, compared to patients with glioblastoma with ¹H-MRS, Pcho/Cr and Pcho/NAA ratios, and NAAG are most important and useful parameters to differentiate between tumoral and normal voxels. Further studies are needed to determine ¹H-MRS ability to differentiate brain tumor region from healthy one.

Acknowledgement

The authors thanks to Kermanshah University of Medical Sciences for providing research funding.

References

1. Tome-Garcia J, Tejero R, Nudelman G, Yong RL, Sebra R, Wang H, et al. Prospective isolation and comparison of human germinal matrix and glioblastoma EGFR+

- populations with stem cell properties. *Stem Cell Reports* 2017;8(5):1421-1429.
2. Al-Saffar NM, Marshall LV, Jackson LE, Balarajah G, Eykyn TR, Agliano A, et al. Lactate and choline metabolites detected in vitro by nuclear magnetic resonance spectroscopy are potential metabolic biomarkers for PI3K inhibition in pediatric glioblastoma. *PLoS One* 2014;9(8):e103835.
 3. Burlina AP, Aureli T, Bracco F, Conti F, Battistin L. MR spectroscopy: a powerful tool for investigating brain function and neurological diseases. *Neurochem Res* 2000;25(9-10):1365-1372.
 4. Smirniotopoulos JG, Murphy FM, Rushing EJ, Rees JH, Schroeder JW. Patterns of contrast enhancement in the brain and meninges. *Radiographics* 2007;27(2):525-551.
 5. Parra NA, Maudsley AA, Gupta RK, Ishkanian F, Huang K, Walker GR, et al. Volumetric spectroscopic imaging of glioblastoma multiforme radiation treatment volumes. *Int J Radiat Oncol Biol Phys* 2014;90(2):376-384.
 6. Xia Y, Yang C, Hu N, Yang Z, He X, Li T, et al. Exploring the key genes and signaling transduction pathways related to the survival time of glioblastoma multiforme patients by a novel survival analysis model. *BMC Genomics* 2017;18(Suppl 1):950.
 7. Crain ID, Elias PS, Chapple K, Scheck AC, Karis JP, Preul MC. Improving the utility of 1H-MRS for the differentiation of glioma recurrence from radiation necrosis. *J Neurooncol* 2017;133(1):97-105.
 8. Ulmer S, Backens M, Ahlhelm FJ. Basic principles and clinical applications of magnetic resonance spectroscopy in neuroradiology. *J Comput Assist Tomogr* 2016;40(1):1-13.
 9. Haaga JR, Boll D. Paul Smith. CT and MRI of the Whole Body, 2-Volume Set. 5th ed. Dogra V, Forsting M, Gilkeson R, Ha KH, Sundaram M (eds). Philadelphia: Mosby, Elsevier; 2009. 2904 p.
 10. Azarakhsh F, Changizi V. Metabolites role in detecting brain tumors using nuclear magnetic resonance spectroscopy and comparing their densities in tumoral patients with those in healthy individuals. *J Payavard Salamat* 2016;10(3):248-257.
 11. Einstein DB, Wessels B, Bangert B, Fu P, Nelson AD, Cohen M, et al. Phase II trial of radiosurgery to magnetic resonance spectroscopy-defined high-risk tumor volumes in patients with glioblastoma multiforme. *Int J Radiation Oncol Biol Phys* 2012;84(3):668-674.
 12. Deviers A, Ken S, Filleron T, Rowland B, Laruelo A, Catalaa I, et al. Evaluation of the lactate-to-N-acetyl-aspartate ratio defined with magnetic resonance spectroscopic imaging before radiation therapy as a new predictive marker of the site of relapse in patients with glioblastoma multiforme. *Int J Radiat Oncol Biol Phys* 2014;90(2):385-393.
 13. Parto Dezfouli MA, Parto Dezfouli M, Ahmadian A, Frangi AF, Esmaili Rad M, Saligheh Rad H. Quantification of 1H-MRS signals based on sparse metabolite profiles in the time-frequency domain. *NMR Biomed* 2017;30(2).
 14. Bottomley PA, Griffiths JR. Handbook of magnetic resonance spectroscopy in vivo: MRS theory, practice and applications. USA: John Wiley & Sons; 2016. 1232 p.
 15. Verma A, Kumar I, Verma N, Aggarwal P, Ojha R. Magnetic resonance spectroscopy-revisiting the biochemical and molecular milieu of brain tumors. *BBA Clin* 2016;5:170-178.
 16. Kreis R. Issues of spectral quality in clinical 1H-magnetic resonance spectroscopy and a gallery of artifacts. *NMR Biomed* 2004;17(6):361-381.
 17. Cianfoni A, Law M, Re TJ, Dubowitz DJ, Rumboldt Z, Imbesi SG. Clinical pitfalls related to short and long echo times in cerebral MR spectroscopy. *J Neuroradiol* 2011;38(2):69-75.
 18. Bertholdo D, Watcharakorn A, Castillo M. Brain proton magnetic resonance spectroscopy: introduction and overview. *Neuroimaging Clin N Am* 2013;23(3):359-380.
 19. Wilson M, Reynolds G, Kauppinen RA, Arvanitis TN, Peet AC. A constrained least-squares approach to the automated quantitation of in vivo 1H magnetic resonance spectroscopy data. *Magn Reson Med* 2011;65(1):1-12.
 20. Biomarkers definitions working group. Biomarkers and surrogate endpoints: preferred definitions and conceptual framework. *Clin Pharmacol Ther* 2001;69(3):89-95.
 21. Kinoshita Y, Yokota A. Absolute concentrations of metabolites in human brain tumors using in vitro proton magnetic resonance spectroscopy. *NMR Biomed* 1997;10(1):2-12.
 22. Righi V, Andronesi OC, Mintzopoulos D, Black PM, Tzika AA. High-resolution magic angle spinning magnetic resonance spectroscopy detects glycine as a biomarker in brain tumors. *Int J Oncol* 2010;36(2):301-306.
 23. Ratai EM, Zhang Z, Fink J, Muzi M, Hanna L, Greco E, et al. ACRIN 6684: multicenter, phase II assessment of tumor hypoxia in newly diagnosed glioblastoma using magnetic resonance spectroscopy. *PLoS One* 2018;13(6):e0198548.
 24. Preul M, Caramanos Z, Collins DL, Villemure JG, Leblanc R, Olivier A, et al. Accurate non-invasive diagnosis of human brain tumors by using proton magnetic resonance spectroscopy. *Nat Med* 1996;2:323-325.
 25. Long PM, Moffett JR, Namboodiri AM, Viapiano MS, Lawler SE, Jaworski DM. N-acetylaspartate (NAA) and N-acetylaspartylglutamate (NAAG) promote growth and inhibit differentiation of glioma stem-like cells. *J Biol Chem* 2013;288(36):26188-26200.
 26. Baslow MH. Functions of N-acetyl-L-aspartate and N-acetyl-L-aspartylglutamate in the vertebrate brain: role in glial cell-specific signaling. *J Neurochem* 2000;75(2):453-459.
 27. Zong H, Parada LF, Baker SJ. Cell of origin for malignant gliomas and its implication in therapeutic development. *Cold Spring Harb Perspect Biol* 2015;7(5). pii: a020610.
 28. Maus A, Peters GJ. Glutamate and α -ketoglutarate: key players in glioma metabolism. *Amino Acids* 2017;49(1):21-32.

29. Elsakka AMA, Bary MA, Abdelzaher E, Elnaggar M, Kalamian M, Mukherjee P, et al. Management of glioblastoma multiforme in a patient treated with ketogenic metabolic therapy and modified standard of care: a 24-month follow-up. *Front Nutr* 2018;5:20.
30. Liubinas SV, O'Brien TJ, Moffat BM, Drummond KJ, Morokoff AP, Kaye AH. Tumour associated epilepsy and glutamate excitotoxicity in patients with gliomas. *J Clin Neurosci* 2014;21(6):899-908.
31. Nelson SJ. Multivoxel magnetic resonance spectroscopy of brain tumors. *Mol Cancer Ther* 2003;2(5):497-507.
32. Kazd T, Bulik M, Pospisil P, Lakomy R, Smrcka M, Slampa P, et al. Advanced MRI increases the diagnostic accuracy of recurrent glioblastoma: Single institution thresholds and validation of MR spectroscopy and diffusion weighted MR imaging. *Neuroimage Clin* 2016;11:316-321.
33. Zeng QS, Li CF, Zhang K, Liu H, Kang XS, Zhen JH. Multivoxel 3D proton MR spectroscopy in the distinction of recurrent glioma from radiation injury. *J Neurooncol* 2007;84(1):63-69.
34. Bulik M, Kazda T, Slampa P, Jancalek R. The diagnostic ability of follow-up imaging biomarkers after treatment of glioblastoma in the temozolomide era: implications from proton MR spectroscopy and apparent diffusion coefficient mapping. *Biomed Res Int* 2015;2015:641023.
35. Roldan-Valadez E, Rios C, Motola-Kuba D, Matus-Santos J, Villa AR, Moreno-Jimenez S. Choline-to-N-acetyl aspartate and lipids-lactate-to-creatine ratios together with age assemble a significant Cox's proportional-hazards regression model for prediction of survival in high-grade gliomas. *Br J Radiol* 2016;89(1067):20150502.
36. Ando K, Ishikura R, Nagami Y, Morikawa T, Takada Y, Ikeda J, et al. [Usefulness of Cho/Cr ratio in proton MR spectroscopy for differentiating residual/recurrent glioma from non-neoplastic lesions]. *Nihon Igaku Hoshasen Gakkai Zasshi* 2004;64(3):121-126. Japanese.
37. Wang Q, Zhang J, Xu W, Chen X, Zhang J, Xu B. Role of magnetic resonance spectroscopy to differentiate high-grade gliomas from metastases. *Tumour Biol* 2017;39(6):1010428317710030.